ADAPTIVE MAXIMUM POWER POINT TRACKING ALGORITHM FOR MULTI-VARIABLE APPLICATIONS IN PHOTOVOLTAIC ARRAYS

✉ Andrés Julián Saavedra Montes[*]
Carlos Andrés Ramos Paja[**]
Luz Adriana Trejos Grisales[***]

ABSTRACT

Classical algorithms for multi-variable photovoltaic systems use fixed-size perturbations, which does not optimize the produced power in both steady-state and transient conditions. Therefore, an adaptive maximum power point tracking algorithm for photovoltaic systems is proposed in this paper to improve the power generation in both transient and steady-state conditions. The proposed algorithm only uses a single pair of current/voltage sensors to reach the global maximum available power, which contrast with the high number of sensors required by others distributed maximum power point tracking solutions. The algorithm recognizes the voltage pattern exhibited by PV system in both steady-state and transient conditions to adapt the size perturbations accordingly: in steady-state conditions reduces the perturbation size to minimize the power loses, while in transient conditions increases the perturbation size to speed-up the tracking of the new operating point. Finally, the adaptive multi-variable perturb and observe algorithm is validated by means of simulation using detailed models.

KEYWORDS: Photovoltaic Generation; Adaptive Algorithm; Maximum Power Point; Efficiency.

ALGORITMO ADAPTATIVO PARA SEGUIMIENTO DEL PUNTO DE MÁXIMA POTENCIA EN APLICACIONES MULTI-VARIABLES DE CAMPOS FOTOVOLTAICOS

RESUMEN

Los algoritmos clásicos para sistemas fotovoltaicos multi-variables usan perturbaciones con amplitud fija, lo cual no optimiza la potencia producida en condiciones estacionarias y transitorias. Por tanto, en este artículo se propone un algoritmo adaptativo para el seguimiento del punto de máxima potencia, el cual incrementa la potencia generada en condiciones estacionarias y transitorias. El algoritmo requiere un único par de sensores de corriente/voltaje para alcanzar el punto de potencia máxima global, en contraste con el alto número de sensores requeridos por otras soluciones distribuidas

[*]   Ingeniero electricista, Magíster en Sistemas de Generación de Energía Eléctrica, Doctor en Ingeniería Eléctrica, Universidad del Valle. Profesor Asociado Universidad Nacional de Colombia, sede Medellín. Medellín (Colombia).

[**] Ingeniero electrónico, Doctor en Ingeniería Electrónica, Automática y Comunicaciones, Universidad Nacional de Colombia, sede Medellín. Profesor Asistente Universidad Nacional de Colombia, sede Medellín. Medellín (Colombia).

[***] Ingenieria electricista, candidata a Doctora en Ingeniería, Universidad Nacional de Colombia, sede Medellín. Medellín (Colombia).

del seguimiento del punto de máxima potencia. El algoritmo reconoce el patrón de voltaje descrito por el sistema fotovoltaico en condiciones estacionarias y transitorias para adaptar el tamaño de las perturbaciones: es condiciones estacionarias reduce el tamaño de las perturbaciones para minimizar las pérdidas de potencia, mientras que en condiciones transitorias incrementa el tamaño de las perturbaciones para acelerar el seguimiento del nuevo punto de operación. Finalmente, el algoritmo es validado a través de simulación utilizando un modelo matemático detallado de un sistema fotovoltaico.

PALABRAS CLAVES: generación fotovoltaica; algoritmo adaptativo; punto de máxima potencia y eficiencia.

ALGORÍTMO ADAPTATIVO PARA RASTREAMENTO DO PONTO DE MÁXIMA POTÊNCIA EM APLICAÇÕES MULTI-VARIÁVEIS DE CAMPOS FOTOVOLTAICOS

SUMÁRIO

Os algorítmos clássicos para sistemas fotovoltaicos multi-variáveis usam perturbações com amplitude fixa, o qual não otimiza a potência produzida em condições estacionárias e transitórias. Por tanto, em este artigo propõe-se um algorítmo adaptativo para o rastreamento do ponto de máxima potência, o qual incrementa a potência gerada em condições estacionárias e transitórias. O algorítmo requer um único par de sensores de corrente/voltaje para atingir o ponto de potência máxima global, em contraste com o alto número de sensores requeridos por outras soluções distribuídas do rastreamento do ponto de máxima potência. O algorítmo reconhece o padrão de voltaje descrito pelo sistema fotovoltaico em condições estacionárias e transitórias para adaptar o tamanho das perturbações: é condições estacionárias reduz o tamanho das perturbações para minimizar as perdas de potência, enquanto em condições transitórias incrementa o tamanho das perturbações para acelerar o rastreamento do novo ponto de operação. Finalmente, o algorítmo é validado através de simulação utilizando um modelo matemático detalhado de um sistema fotovoltaico.

PALAVRAS-CHAVE: Geração fotovoltaica; Algorítmo adaptativo; Ponto de máxima potência e eficiência.

1. INTRODUCTION

Photovoltaic (PV) power systems provide electrical power in agreement with the solar irradiance and temperature acting on the PV modules as reported by Femia, *et al.* (2009) and Femia, *et al.* (2005). Therefore, a large amount of possible operating points can occur since multiple environmental conditions can be present in different modules of the PV array as presented by Femia, *et al.* (2008).

In addition, each PV module can operate in multiple operation conditions as observed in figure 1, where the experimental electrical characteristics of a BP585 PV panel, composed by two PV modules, are reported for two different irradiances. Such a figure also depicts the electrical behavior simulation of the BP585 module by means of the PV model reported by Petrone and Ramos-Paja (2011). From figure 1 is evident that an optimal point exists, named Maximum Power Point (MPP), in which the

PV panel produces the maximum power available for the particular environmental conditions.

Several search algorithms, named Maximum Power Point Tracking (MPPT) algorithms, have been proposed in literature by Subudhi and Pradhan (2013) to find the MPP. Among them, the Perturb and Observe (PO) algorithm reported by Femia, *et al.* (2005), Femia, *et al.* (2009) is the most widely adopted due to its simplicity and satisfactory performance. Such a solution perturbs the PV voltage in the direction that increases the PV power, where classical implementations define the perturbation size to provide a trade-off between tracking speed and steady-state power losses: large perturbation sizes provide fast tracking of a new MPP, but also generate high steady-state power losses due to the large oscillation around the MPP; instead, short perturbation sizes provide small steady-state power losses, but due to the small power in the perturbed variable, the transition to a new MPP is slow, generating additional power losses.

Figure 1. Electrical characteristics of a BP585 PV panel

(a) Current-voltage curves

(b) Power-voltage curves
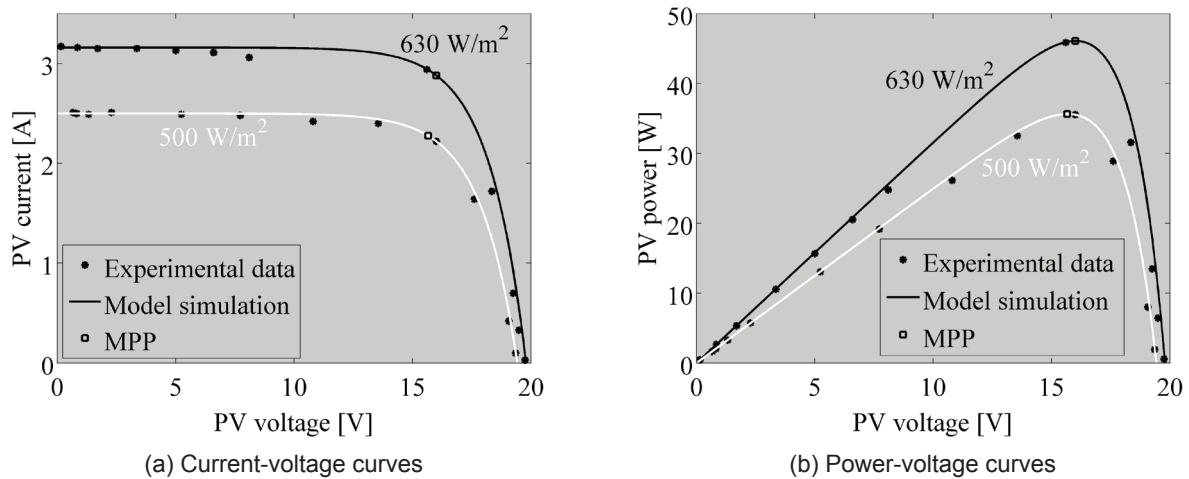
Such a problem was addressed by Femia, *et al.* (2007) and Piegari and Rizzo (2010), where the new position of the MPP is predicted using the PV model, which parameters are estimated online, and the perturbation size is modified to match the predicted MPP voltage. The main drawback of such solutions concerns the error introduced by the model estimation, which can be further affected by environmental changes after the parameters estimation. A different approach was proposed by Abdelsalam, *et al.* (2011), where the perturbation size is modified in agreement with the power difference between consecutive perturbation cycles: a PI controller is used to modify the perturbation size in the direction that minimized the power differences. Similarly, the solution reported by Lee and Kim (2012) uses a parameterized equation to dynamically modify the perturbation size based on the PV panel operating point. Since both solutions require a parameterized equation, it is evident that an off-line parameterization is required, which increases the solution complexity and implementation time. Instead, the solution proposed by Jiang, *et al.* (2013), uses the derivative between the perturbed and observed variables to define the perturbation size, it aiming for the size that reduces such a derivative. This solution is less dependent from the system parameters, which makes it more reliable and simple to implement. But all of those solutions proposed by Femia, *et al.* (2007), Piegari and

Rizzo (2010), Abdelsalam, *et al.* (2011), Lee and Kim (2012), Jiang, *et al.* (2013) consider the action on a single variable, which is the case of classical centralized MPPT algorithms. Such a condition generates large power losses when some modules in the PV array are subjected to different conditions (mismatching), this because multi-peaks occur in the power vs. voltage curve, each one of them with lower power than the sum of the modules maximum power as reported by Femia, *et al.* (2008). In addition, such centralized MPPT approaches can be trapped in a peak (maximum) that could not be the highest one.

To avoid the large drops of centralized PV systems in mismatching conditions, the concept of Distributed Maximum Power Point Tracking (DMPPT) algorithm is introduced by Femia, *et al.* (2008): each PV module is controlled independently by means of a dedicated power converter and MPPT algorithm, while the output power is aggregated into the load. Such a solution avoids the multi-peaks problem, but introduces the requirement of as many current/voltage pair of sensors and MPPT processing devices as PV modules. This drawback was addressed in Petrone, *et al.* (2012), where a single current/voltage pair of sensor and a single MPPT processing device is required for any number of PV modules. But the design of both Femia, *et al.* (2008) and Petrone, *et al.* (2012) solutions consider a fixed step perturbation, which generates the same contradictory behavior between

tracking speed and steady-state power losses present in the classical PO algorithm.

Therefore, this paper proposes a DMPPT algorithm with adaptive perturbation size, which is aimed at improving the power generation in both transient and steady-state conditions. The proposed solution is based on the DMPPT idea introduced by Petrone, *et al.* (2012), but considering an asynchronous modification of the perturbation size for all the PV modules. In addition, the proposed adaptive technique is based on the novel idea of reducing the perturbation size when the PV system is in steady-state conditions, and increasing it in other transient conditions. This solution does not require any model or parameters estimation, or derivative calculation, since it is based on the pattern recognition of stable PO profiles. Hence, the proposed DMPPT algorithm improves the power extraction from PV arrays, and it is more reliable and easy to implement than both classical solutions for DMPPT and adaptive algorithms.

2. ADAPTIVE PERTURBATION BASED ON PATTERN RECOGNITION

The classical PO algorithm, as many other classical algorithms reported by Subudhi and Pradhan (2013), acts directly on the duty cycle D of a dc/dc converter or indirectly on the reference V_{ref} of a closed-loop PV voltage control. The PO algorithm is designed by means of two parameters: the perturbation period Ta and the perturbation size ΔM. The former is defined to be larger than the PV system settling time, which in open loop (perturbing D) is imposed by the dc/dc converter passive elements, while in closed loop (perturbing V_{ref}) is imposed by the control system Femia, *et al.* (2009). In both cases, the time interval Ta between the signal perturbation and the analysis of its effect must be larger, or at least equal, to the system settling-time, otherwise the MPPT algorithm will observe a transient power different from the steady-state value, and the subsequent decision will be based on incorrect information leading to a wrong operation as described by Femia, *et al.* (2009) and Femia, *et al.* (2005). Despite Jiang, *et al.* (2013) proposes to dynamically modify Ta, such a feature does not impact the power losses in a significant way: if ΔM is large enough, the tracking of a new MPP is fast, which

reduces the transient power losses; while if ΔM is small enough, the steady-state oscillation around the MPP is also small, which reduces the steady-state power losses. Therefore, as adopted in Femia, *et al.* (2007), Piegari and Rizzo (2010), Abdelsalam, *et al.* (2011), Lee and Kim (2012), the modification of ΔM with a fixed Ta is enough to implement an adaptive MPPT algorithm.

Figure 2 illustrates the impact of ΔM in the performance of the PO algorithm: figure 2(a) shows both transient and steady-state behaviors for a large ΔM, while figure 2(b) shows both transient and steady-state behaviors for a small ΔM. In the first condition, the tracking of the MPP takes 11 steps, while in the second condition the same MPP is reached in 23 steps. Such a difference put in evidence the increased tracking speed provided by large ΔM values. But, in contrast, **Figure 2(a)** and **Figure 2(b)** show that large ΔM values produce large oscillations around the MPP, while small ΔM values guarantee a behavior near the MPP, which increases the power extracted from the PV. **Figure 2(c)** illustrates the increased power profile generated by the fast MPP tracking provided by large ΔM values, while **Figure 2(d)** illustrates the additional power losses generated by large ΔM values in steady-state conditions. Therefore, large ΔM values are required to track a new MPP in transient conditions, while small ΔM values are required for steady-state environmental conditions.

In addition, **Figure 2(a)**, **Figure 2(b)**, and **Figure 2(c)** show the voltage profiles generated by the PO algorithm in steady-state conditions, where three voltage levels appear: a first voltage level lower than the MPP, which in **Figure 2(a)** and **Figure 2(b)** is at the left of the MPP and in figure 2(d) is below the MPP; a second voltage level near the MPP; and a third voltage level higher than the MPP, which in **Figure 2(a)** and **Figure 2(b)** is at the right of the MPP and in **Figure 2(d)** is over the MPP. Such a steady-state profile known as the three-point behavior guarantees a correct steady-state PO operation.

Therefore, this work is based on the detection of the three-point behavior to dynamically modify the ΔM value: if the steady-state pattern is detected, ΔM value is reduced until a minimum value is reached; while if the steady-state pattern is not detected, ΔM value is increased until a maximum value is reached.

Figure 2. Transient and steady-state behavior of PO algorithm

(a) Large DM parameter

(b) Small DM parameter

(c) Transient profile

(d) Steady-state profile
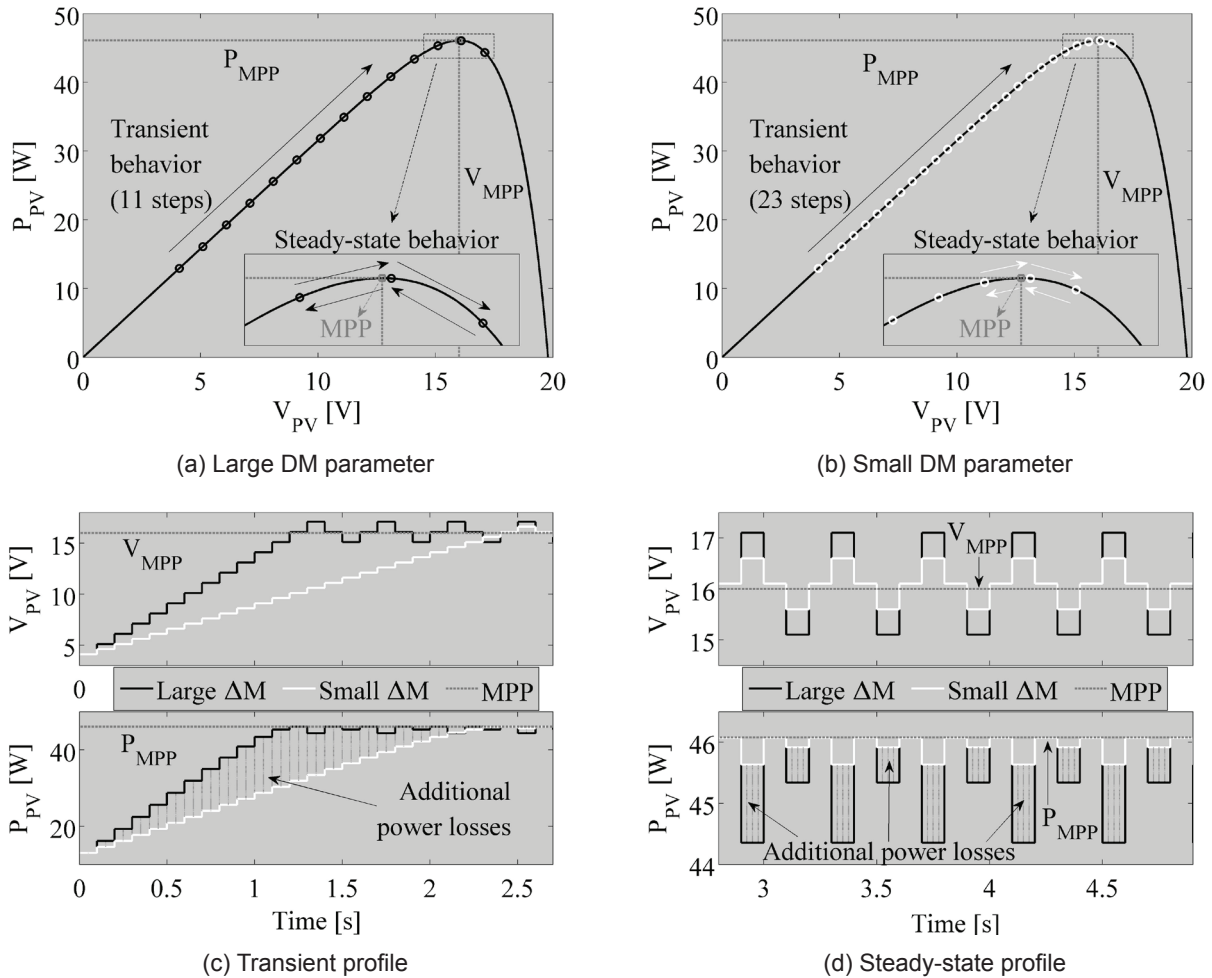
2.1 Pattern Recognition of the Three-Point Behavior

To detect the steady-state operation of the PV system, the PO three-point behavior (TPB) on the manipulated variable, duty-cycle or reference voltage, must be recognized. In the proposed solution, such a procedure is performed by the *TPB detector*, which inspects the output of the PO algorithm, signal M, following the flowchart given at the left of **Figure 3**: the PO signal is acquired every perturbation cycle, and its present value M(k) is compared with the previous one M(k-1) to detect if the signal exhibits a rising edge, F(k) = 1, or a falling edge,

F(k) = 0. Then, the last M flanks are stored in a vector Fv = [F(k), F(k-1), F(k-2), F(k-3)] that is further analyzed.

Since the steady state profile of the TPB is characterized by an oscillation around the MPP, as depicted in **Figure 2(d)**, three levels are present in M: low, medium and high. The TPB is the following: low, medium, high, medium, low, etc., which can be described in terms of the flanks as: Fv = [1,1,0,0], therefore the TPB is defined by four flanks. But depending on the first observed TPB element different profiles are obtained: starting on the first low Fv = [1,1,0,0], starting on the first medium Fv = [1,0,0,1], starting on high Fv = [0,0,1,1], and starting on the

second medium Fv = [0,1,1,0]. The last example is illustrated in the right side of **Figure 3**, where Fv is constructed with the flanks that occur after the second medium level of M. Moreover, from the previous analysis it is noted that the TPB, expressed in terms of flanks, exhibits two consecutive flanks of the same value, i.e. [1,1] or [0,0]. Therefore, as described in the flowchart of figure 3, the PO is in steady state (SS = 1) if Fv has two consecutive elements with the same value, i.e. [1,1] or [0,0], otherwise the PO is in transient condition (SS = 0).

2.2 Perturbation Size Modification

From the previous analysis concerning the optimization of the PO algorithm by modifying the amplitude of M perturbations ΔM, if the PO algorithm is in steady-state (SS = 1) the amplitude ΔM must be decreased, otherwise if the PO algorithm is in transient conditions (SS = 0) the amplitude ΔM must be increased. Such a procedure is performed, by the *ΔM modifier*, using the information generated by the TPB detector following the flowchart given in the left side of **Figure 4**, where ΔM is modified in a magnitude ΔM depending on the SS value.
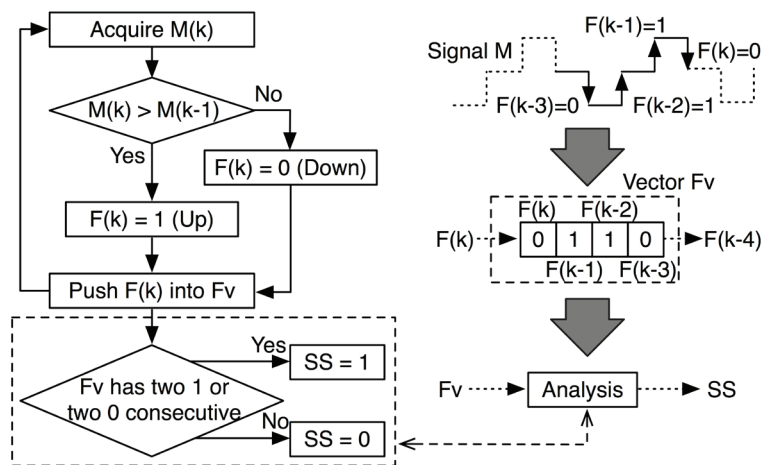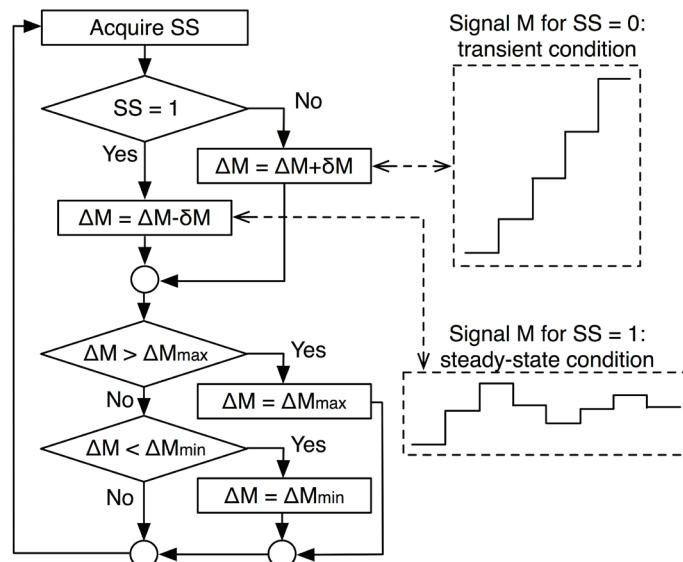
Figure 3. TPB detector flowchart

Figure 4. DM modifier flowchart

Moreover, the maximum and minimum values of ΔM are constrained to ΔM_{max} and ΔM_{min}, respectively. The right side of figure 4 illustrates the transient and steady-state profiles of the PO algorithm under the action of the ΔM modifier: signal M is increased to track the MPP, while M is decreased around the MPP to reduce the power losses due to the PO oscillation.

To dynamically modify ΔM the three components of the proposed Adaptive PO (APO) must be operated together: the TPB detector must to detect whenever the PO algorithm operates in steady-state, the ΔM modifier must to adjust ΔM to reduce the PO power losses, and the PO must to track the MPP. The structure proposed to implement the APO is depicted in **Figure 5**, which without loss of generality is based on a Boost converter interacting with a dc-link, while a Norton equivalent represents the PV module. Such source and load representations are widely adopted in PV systems, and both have been extensively analyzed by Trejos, *et al.* (2012).

In such a structure the APO provides the control signal M to the *Modulator* that drives the dc/dc converter, which could be a PWM circuit as in Femia, *et al.* (2005) or a voltage control loop as in Femia, *et al.* (2009). Moreover, the proposed APO requires four parameters: the perturbation period Ta, ΔM_{min}, ΔM_{max} and ΔM.

The open loop transfer function of the Boost-based PV system, calculated in Trejos, *et al.* (2012), is given in (1). To ensure a TPB on the PO algorithm, Ta must be larger than the setting time of such a PV system. Therefore, Femia, *et al.* (2005) proposes (2) to calculate Ta in the cases where a PWM is adopted,

ε= 0,1 corresponds to a 10 % band, but other settling time bands can be assumed, e.g. 2 % and 5 % bands. Otherwise, where a voltage controller is adopted as modulator, Femia, *et al.* (2009) proposes to set Ta larger than the settling time of the PV voltage measured in closed loop.

$$G_{pv}(s) = \frac{-R_{MPP} \cdot V_b}{L \cdot C \cdot R_{MPP} \cdot s^2 + L \cdot s + R_{MPP}} \qquad 1)$$

$$T_a \geq -2 \cdot R_{MPP} \cdot C \cdot h(\varepsilon) \qquad (2)$$

The lower limit ΔM_{min} of ΔM must be defined to obtain a perturbation on the PV power δP_{pv} larger than the power ripple δP_{pv} generated by the switching operation of the dc/dc converter. The $\delta P_{pv} > \Delta P_{pv}$ condition guarantees that the PO algorithm of figure 5 makes decisions only based on ΔM, otherwise the PO algorithm can be confused by the effects of the PV voltage ripple on the PV power. Such a procedure is described in detail in Femia, *et al.* (2005) for a PO controller perturbing the duty cycle by means of a PWM, while Femia, *et al.* (2009) describes the same procedure for a PO controller perturbing the PV voltage reference of a modulator based on a feedback controller.

The maximum value of ΔM, i.e. ΔM_{max}, must be defined to avoid an excessive oscillation of M when the algorithm reaches the MPP. This work considers

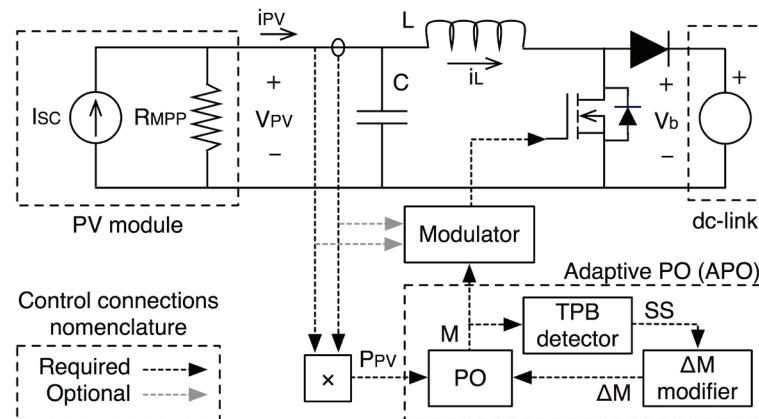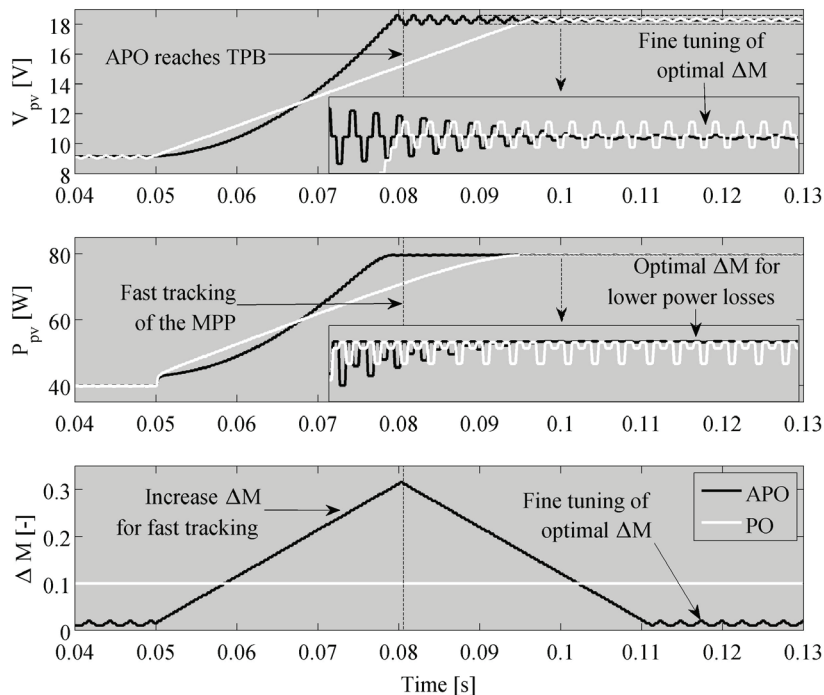Figure 5. PV system based on a dc/dc converter controlled by the APO

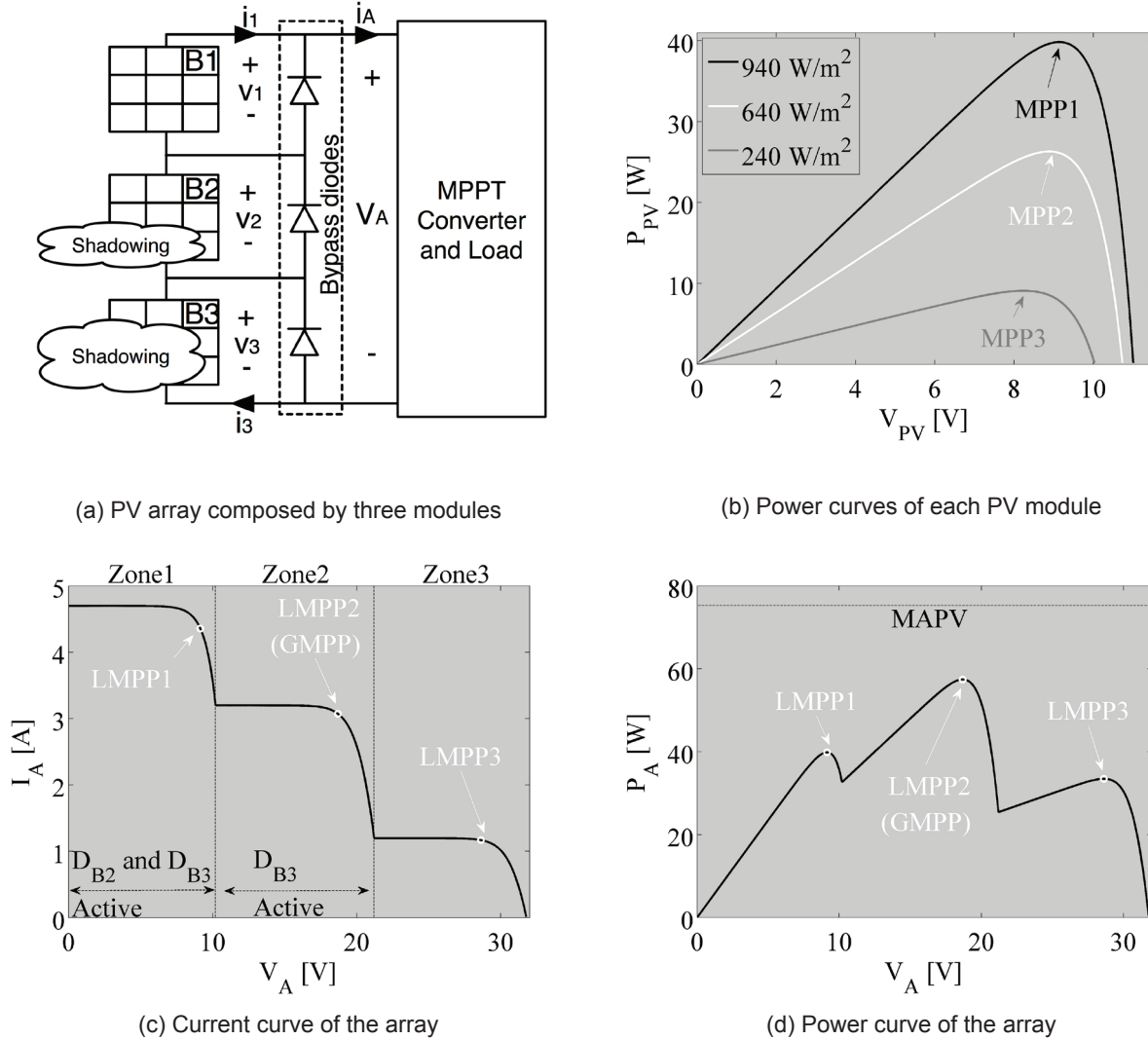**Figure 6.** APO and traditional PO comparison in both transient and steady-state conditions

a $\Delta M_{max} = 50 \cdot \Delta M_{min}$ to illustrate the solution behavior with a large excursion of ΔM, but any other value can be adopted. In a similar way, ΔM must be defined in a trade off between tracking speed and converge to the optimal ΔM: large ΔM provides a fast tracking of a new MPP, but such large ΔM value avoids a fine tuning of the optimal ΔM value. Instead, small ΔM allows to accurately detecting the best ΔM value, but in contrast the tracking of the MPP is slow due to the small changes on ΔM. This work considers a $\Delta M = \Delta M_{min}/2$ to provide trade off between tracking speed and converge to the optimal ΔM, however any other value can be adopted.

To illustrate the advantages of the proposed APO over the classical PO, both the APO and PO algorithms were simulated acting on a voltage controlled Modulator; where $\Delta M_{min} = 10$ mV, Ta = 0,5 ms and the PO fixed perturbation $\Delta M_{PO} = 10 \cdot \Delta M_{min}$ were designed following the guidelines given in Femia, *et al.* (2009). **Figure 6** shows the algorithms simulation: both algorithms start in steady-state conditions, and at 0.05 s an irradiance step generates a change on the MPP that must be tracked.

The simulation results of **Figure 6** put in evidence the improved tracking speed provided by the APO in comparison with the PO, where the APO reaches the new MPP (denoted by a TPB) after 31 ms, while the PO reaches the same MPP after 47 ms, which means that the PO requires 50 % more time. Such an improved tracking speed is achieved due to the increment in ΔM generated by the ΔM modifier when SS = 0 is detected. Similarly, the zoom of figure 6 in both PV voltage V_{pv} and power P_{pv} show the convergence of ΔM to an optimal value generated by the APO, where ΔM is decreased in SS = 1 conditions to reduce the steady-state power losses, which are much smaller than the steady-state losses generated by the PO. Finally, the simulation results put in evidence the improved transient and steady-state behavior of the APO solution: it tracks faster the MPP for changes on the environmental conditions, but it generates lower losses in steady-state conditions; therefore the APO increases the power extracted from a PV source in comparison with the traditional PO.

Figure 7. Mismatching conditions and multiple maximums in PV arrays

(a) PV array composed by three modules

(b) Power curves of each PV module

(c) Current curve of the array

(d) Power curve of the array

3. MISMATCHING CONDITIONS AND DISTRIBUTED ALGORITHM

The previous APO algorithm acts on a single variable, thus it is subjected to the same problems of the PO acting on a PV array in mismatching conditions, which could be trapped in a suboptimal maximum power or Local MPP (LMPP) instead of the global MPP (GMPP). But it must be point out that all the LMPP in an array, including the GMPP, exhibit an array power lower than the Maximum Available PV (MAPV) power, which cor-

responds to the sum of all the MPP powers available in each PV module.

To illustrate such concepts, a PV array composed by the series connection of three BP585 PV modules is adopted, which scheme is depicted in **Figure 7(a)**. It is important to note that such a series array, named string, requires diodes in anti-parallel with each module to prevent degradation in mismatching conditions as reported in Petrone and Ramos-Paja (2011). Since the modules are connected in series its current is defined by the lower PV current, which depends on the irradiance

conditions. Hence, the modules with high irradiance will dissipate by means of heat the current in excess, producing artificial aging and hot-spots that degrade such modules. To prevent those undesired conditions, the anti-parallel diodes, named bypass diodes, provide an alternative path to the difference between the larger current of the modules with higher irradiance and the smaller current of the modules with lower irradiance. In such a new condition, the string current is defined by the higher PV current, where the activation of a bypass diode imposes a short-circuit condition to the associated PV module, imposing a null power production to such a module.

The scheme **Figure 7(a)** also includes a MPPT controller and a dc/dc converter that interacts with the load, which consists in a grid-connected inverter. Since such a MPPT technique perturbs the array voltage only, it represents a centralized solution or CMPPT. **Figure 7(b)** shows the power curves of each PV module, where the corresponding MPPs are observed. Taking into account that the PV modules operate in a series connection, **Figure 7(c)** and **Figure 7(d)** show the string current and power curves. There are observed three different LMPP, where LMPP2 corresponds to the GMPP, and as anticipated before, all the LMPP exhibit lower power than the MAPV. Such a condition is generated by the action of the bypass diodes, since its activation deactivates the associated PV module. In example, in the Zone 1 of **Figure 7(c)** the bypass diodes associated to the second and third modules, named D_{B2} and D_{B3} respectively, are active since both modules have lower current than the first one. Instead, in Zone 2, D_{B3} is the only one active because the string current is lower than the PV current of the first and second modules, while the current of the third module stills smaller than the string current. Finally, in Zone 3 there is not active any bypass diode.

To overcome the power drop generated by the bypass diodes in mismatching conditions while protecting the PV modules, Femia, *et al*. (2008) proposed the Distributed Maximum Power Point Tracking or DMPPT.

3.1 Distributed Maximum Power Point Tracking

The main concept of DMPPT structure is to replace the bypass diodes by dc/dc converters. In such a condition each PV module is isolated from the other ones, thus there is no possibility of currents in excess

that produce artificial aging or hot-spots, protecting in this way the modules as reported by Femia, *et al*. (2008). Moreover, since the dc/dc converters are able to impose the PV voltage to the associated PV module, the system is able to operate at the MPP of each module to achieve the MAPV power, providing more power to the load in comparison with CMPPT solutions like the traditional PO interacting with PV arrays protected by means of bypass diodes.

But the DMPPT topology introduced by Femia, *et al*. (2008) considers a traditional PO controller for each dc/dc converter. Therefore a pair of current/voltage sensors and a processing unit is required for each PV module, increasing the cost and complexity of the solution. Moreover, the operating points of the dc/dc converters were not taken into account for the output power maximization, which could introduce significant losses. Such aspects were addressed by Petrone, *et al*. (2012) by means of a multi-output DMPPT algorithm named MVPO, where the basic idea was to maximize the power at the output of the dc/dc converters instead of at the PV terminals. Moreover, a single DMPPT controller was used to generate the control signals for all the dc/dc converters following the structure given in **Figure 8**, where N PV modules are controlled and the load block represents a grid-connected inverter.

The MVPO solution reduces the number of pair of current/voltage sensors and processing units to 1 pair of sensors and 1 processing unit, and also takes into account the dc/dc converters' operating point in the optimization process. Such characteristics improve the extraction of PV power in comparison with the solution presented by Femia, *et al*. (2008). But since the MVPO uses a fixed ΔM value, in the same way that the classical PO, it is impossible to guarantee both fast transient behavior and low steady-state power losses. Therefore, this paper proposes to extend the APO algorithm to act on multiple dc/dc converters, obtaining an Adaptive Multi-Variable PO (AMPO) algorithm for DMPPT applications.

3.2 Adaptive Multi-Variable PO (AMPO) Algorithm

To extend the APO to perform DMPPT in multiple PV modules, the new AMPO algorithm perturbs a single

Figure 8. DMPPT structure with a multi-output DMPPT algorithm
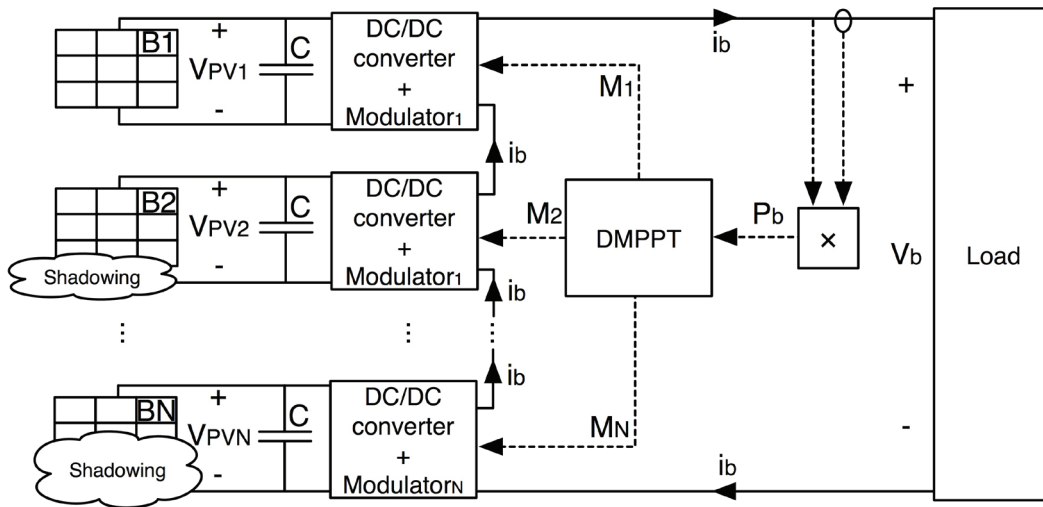
variable at any time, thus the algorithm is able to detect the effect on the output power of changes in a particular module. With such a characteristic the AMPO solution requires a single pair of current/voltage sensors to generate all the control signals for the associated dc/dc converters. Figure 9 shows the block diagram of the proposed AMPO algorithm, where N modulator signals are generated to maximize the power extraction on N PV modules.

From such a block diagram it is noted that the AMPO measures the output power P_b (see **Figure 8**), which is processed by the MVPO algorithm to generate N control signals. Each control signal is analyzed by the TPB detector to recognize which modules are in steady-state and which of them are in transient conditions. Then, using such information, the amplitude of each control signal is changed by the ΔM modifier block to speed-up the tracking of the MAPV operating point and to minimize the steady-state power losses. Moreover, since the AMPO drives multiple PV modules, it generates a control signals vector Mv and a perturbation amplitudes vector ΔMv, where each element of such vectors correspond to a modulator control signal of a particular dc/dc converter as depicted in **Figure 9.**

In addition, it is noted that the AMPO modifies a single control signal at any time, while the other control signals remains constant. To illustrate such a condition, the AMPO flowchart is given in figure 10. If output power increases due to last perturbation, the control signal of the module previously perturbed is changed again in the same direction. Otherwise, if output power decreases, the control signal of the module previously perturbed is kept constant, and the AMPO affects the control signal of other PV module in an opposite direction with respect to the last perturbation performed in that module. Such a procedure is managed using the counter idx to identify the module to be perturbed. In addition, idx is used to access the corresponding signal M_i and amplitude ΔM_i in vectors Mv and ΔMv, respectively.

Figure 10 also shows interaction with TPB detector block. TPB detector inspects the control signal Mv(idx) of the module currently perturbed (defined by idx) to generate the SS signal, where SS = 1 means steady-state. Such information is then processed by ΔM modifier block, the amplitude ΔMv(idx) of signal Mv(idx) is decreased to fine-tuning the MPP detection, otherwise ΔMv(idx) is increased to speed-up the tracking of the new MPP. It is noted that the ΔM modifier generates ΔMv vector where a single component is changed at any time.

3.3 AMPO Algorithm Validation

To validate the proposed AMPO algorithm, a realistic PV system model was adopted. Such a system, which electrical scheme is depicted in **Figure 11**, is composed by three BP585 PV modules, each one of them associated to a dc/dc Boost converter, where the converters' outputs are connected in series to provide a large output voltage. Moreover, the PV system interacts

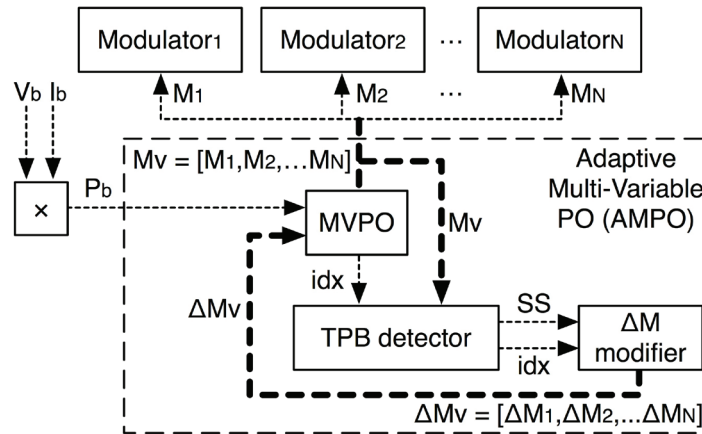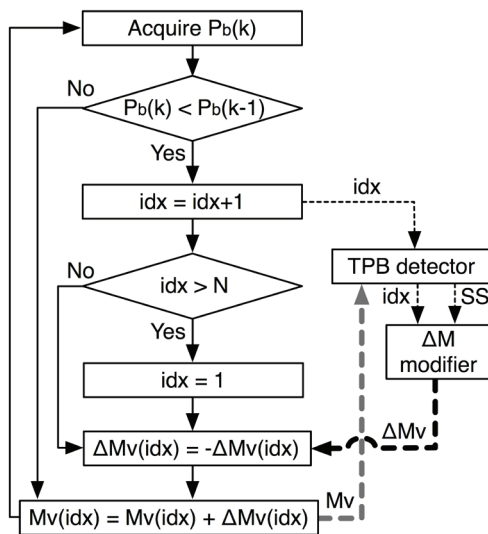**Figure 9.** Block diagram of the AMPO algorithm

Figure 10. Flowchart of the AMPO algorithm

with a dc-bus simulated by means of a Thevenin model, which is a widely adopted model for inverters and battery charges as presented by Trejos, *et al*. (2012), Femia, *et al*. (2008), Femia, *et al*. (2009). In addition, the input voltages of the dc/dc converters are regulated by means of PID controllers as described by Trejos, *et al*. (2012), which reference is defined by the power maximization algorithm, e.g. MVPO or AMPO. The MVPO algorithm implementation is described by Petrone, *et al*. (2012), while the AMPO components presented in **Figure 9** were implemented in the MV_MPPT (MVPO) and SS_and_Modi (TPB detector and ΔM modifier) blocks.

The simulation presented in figure 12 considers a starting PV voltage equal to 5 V for all the modules, it adopting an irradiance of 1.000 W/m^2 that imposes a MPP voltage equal to 9,1 V. The first simulation was performed with the MVPO controlling the PV system (top traces), where the algorithm drives the PV voltages to the MPP one module at the time with a fixed voltage perturbation, it taking 0,42 s to reach a steady-state condition around the MAPV operating point. Instead, the second simulation was performed with the proposed AMPO controlling the PV system (middle traces), where the algorithm uses a variable PV voltage perturbation to reach a steady-state condition around the MAPV operating point in 0,19 s, it representing 54 % less time in transient condition, which highlights the faster tracking of the new MPP provided by the AMPO. In addition, it is observed the perturbation size reduction performed by the AMPO when it reaches TPB, which reduces the steady-state power losses as previously demonstrated.

Finally, the power profiles of both MVPO and AMPO are presented in the bottom traces, where the high power production of the proposed AMPO solution is evident. In such a simulation, the MVPO produces 42,71 J in the transient between 0,0051 s and 0,4230 s (time taken by MVPO to reach TPB); while the AMPO produces 48 J in the same time interval, which represents an improvement of 12,38 % in the energy production just by using AMPO instead of MVPO. Such results put in evidence the correctness of the proposed solution, and also they illustrate the advantages of AMPO over the recently published MVPO.

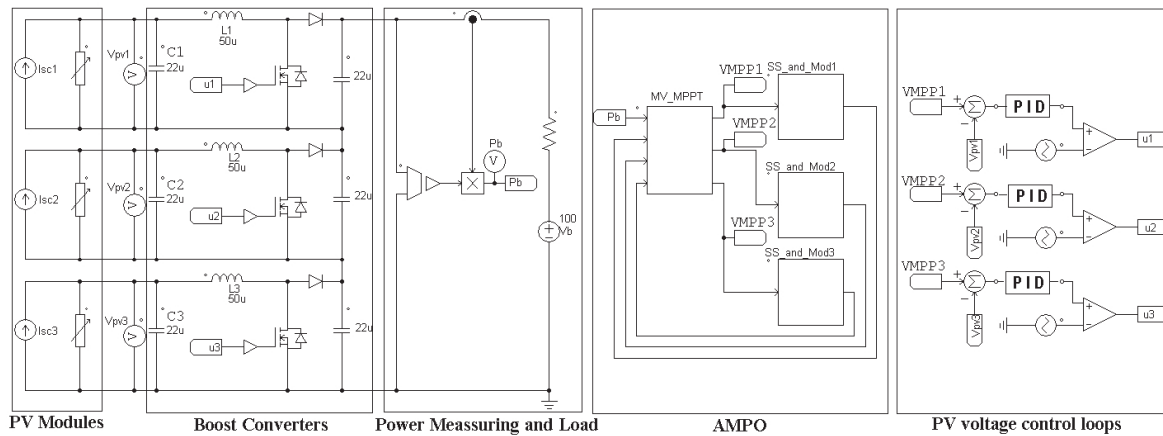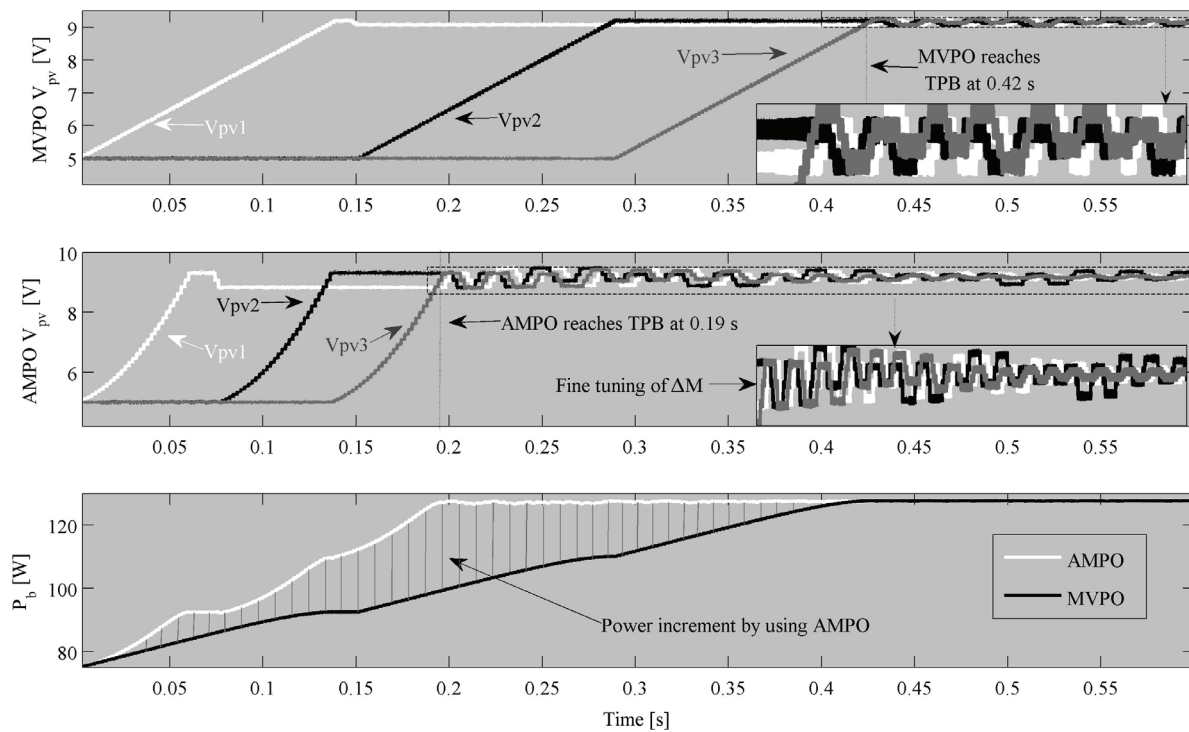**Figure 11.** Electrical scheme implemented in PSIM

Figure 12. Simulation of both AMPO and MVPO algorithms

4. CONCLUSIONS

This paper proposes the adaptive multi-variable PO algorithm AMPO to perform a distributed maximum power point tracking on several PV modules. The algorithm is based on the detection of the steady-state profile TPB on each PV module. When a module exhibits TPB means that such a module is operating at its MPP, therefore the perturbations on the PV voltage must be decreased to reduce the power losses caused by the oscillation around the MPP. Otherwise, the perturbations on the PV voltage must be increased to reach the MPP as fast as possible, this to increase the total power extracted from the module. Moreover, the AMPO perturbs asynchronously each PV module of the array to detect the effect of each module on the total output power. Such conditions make possible to use a

single pair of current/voltage sensors to reach the global maximum available MAPV power, which contrast with the high number of sensors required by a DMPPT solution composed by multiple PO. In addition, due to the adaptive nature of the AMPO, it is much faster in the tracking of the MAPV in comparison with other multi-output algorithms such as the MVPO solution. Similarly, the AMPO reaches the minimum amplitudes of the modules perturbations allowed in steady-state, which reduces the power losses in comparison with fixed-size perturbations algorithms such

as the MVPO algorithm. Finally, the AMPO solution was validated by means of simulations using detailed models.

5. ACKNOWLEDGMENTS

REFERENCES

Abdelsalam, A. K.; Massoud, A. M.; Ahmed, S. and Enjeti, P. N. (2011). High-Performance Adaptive Perturb and Observe MPPT Technique for Photovoltaic-Based Microgrids. *IEEE Transactions on Power Electronics,* 26(4), pp 1010-1021.

Femia, N.; Granozio, D.; Petrone, G. and Vitelli, M. (2007) Predictive & Adaptive MPPT Perturb and Observe Method. *IEEE Transactions on Aerospace and Electronic Systems,* 43(3), pp 934-950.

Femia, N.; Lisi, G.; Petrone, G.; Spagnuolo, G. and Vitelli, M. (2008). Distributed Maximum Power Point Tracking of Photovoltaic Arrays: Novel Approach and System Analysis. *IEEE Transactions on Industrial Electronics,* 55(7), pp 2610-2621.

Femia, N.; Petrone, G.; Spagnuolo, G. and Vitelli, M. (2005) Optimization of perturb and observe maximum power point tracking method. *IEEE Transactions on Power Electronics,* 20(4), pp 963-973.

Femia, N.; Petrone, G.; Spagnuolo, G. and Vitelli, M. (2009). A Technique for Improving P&O MPPT Performances of Double-Stage Grid-Connected Photovoltaic Systems. *IEEE Transactions on Industrial Electronics,* 56(11), pp 4473-4482.

Jiang, Y.; Abu Qahouq, J. A. and Haskew, T. A. (2013) Adaptive Step Size With Adaptive-Perturbation-Frequency Digital MPPT Controller for a Single-Sensor Photovoltaic Solar System. *IEEE Transactions on Power Electronics,* 28(7), pp 3195-3205.

Lee, K.-J. and Kim, R.-Y. (2012). An Adaptive Maximum Power Point Tracking Scheme Based on a Variable Scaling Factor for Photovoltaic Systems. *IEEE Transactions on Energy Conversion,* 27(4), pp 1002-1008.

Petrone, G. & Ramos-Paja, C. A. (2011). Modeling of Photovoltaic Fields in Mismatched Conditions for

Energy Yield Evaluations. *Electric Power Systems Research,* 81 (4), pp 1003-1013.

Petrone, G.; Ramos-Paja, C. A.; Spagnuolo, G. and Vitelli, M. (2012). Granular Control of Photovoltaic Arrays by Means of a Multi-Output Maximum Power Point Tracking Algorithm. *Progress in Photovoltaics: Research and Applications, Article in Press, DOI: 10.1002/pip.2179.*

Piegari, L. and Rizzo, R. (2010). Adaptive Perturb and Observe Algorithm for Photovoltaic Maximum Power Point Tracking. *IET Renewable Power Generation,* vol. 4(4), pp 317-328.

Subudhi, B. and Pradhan, R. (2013). A Comparative Study on Maximum Power Point Tracking Techniques for Photovoltaic Power Systems. *IEEE Transactions on Sustainable Energy,* 4, pp 89-98.

Trejos, A.; González, D. and Ramos-Paja, C. A. (2012) Modeling of Step-up Grid-Connected Photovoltaic Systems for Control Purposes. *Energies,* 5(6), pp 1900-1926.